

Wireless Powered Cognitive Radio Networks with Compressive Sensing and Matrix Completion

Zhijin Qin, Yuanwei Liu, Yue Gao, Maged ElKashlan, and Arumugam Nallanathan

Abstract—In this paper, we consider cognitive radio networks in which energy constrained secondary users (SUs) can harvest energy from the randomly deployed power beacons (PBs). A new frame structure is proposed for the considered networks. In the considered network, a wireless power transfer (WPT) model is proposed, and the closed-form expressions for the power outage probability are derived. Additionally, in order to reduce the energy consumption at SUs, sub-Nyquist sampling are performed at SUs. Subsequently, compressive sensing and matrix completion techniques are invoked to recover the original signals at the fusion center, by utilizing the sparsity property of spectral signals. Throughput optimizations of the secondary networks are formulated into two linear constrained problems, which aim to maximize the throughput of a single SU and the whole cooperative network, respectively. Three methods are provided to obtain the maximal throughput of secondary networks by optimizing the time slots allocation and the transmit power. Simulation results show that the maximum throughput can be improved by implementing compressive spectrum sensing in the proposed frame structure design.

Keywords: Compressive sensing, matrix completion, spectrum sensing, sub-Nyquist sampling, wireless power transfer.

I. INTRODUCTION

ENERGY efficiency and spectrum efficiency are two critical issues in designing wireless networks. Recent developments in energy harvesting provides a promising technique to improve the energy efficiency in wireless networks. Different from harvesting energy from traditional energy sources (e.g., solar, wind, water, and other physical phenomena) [1], the emerging wireless power transfer (WPT) further underpins the trend of green communications by harvesting energy from radio frequency (RF) signals [2]. Inspiring by the great convenience offering by WPT, several works have been studied to investigate the performance of different kinds of energy constraint networks [3]–[7]. Two practical receiver architectures, namely a time switching receiver and a power splitting receiver [8], were proposed in a multi-input and multi-output (MIMO) system in [3], which laid a foundation in the recent research of WPT. In [4], a new hybrid network architecture is designed to enable charging mobiles wirelessly in cellular networks. In [5], three wireless power transfer schemes were proposed for secure device-to-device (D2D) communication scenarios. For cooperative systems, new power allocation strategies are proposed in a cooperative networks

where multiple sources and destinations are communicated by an energy harvesting relay in [6]. For non-orthogonal multiple access (NOMA) networks, a new cooperative simultaneously wireless information and power transfer NOMA protocol is proposed with considering the scenario where all users are randomly deployed in [7].

Along with improving energy efficiency through energy harvesting, wideband cognitive radio (CR) technique can improve the spectrum efficiency and capacity of wireless networks through dynamic spectrum access [9]. More particularly, the secondary users (SUs) in CR networks (CRNs) are normally energy constrained and powered by battery. Therefore, SUs are normally critical to energy consumption in order to increase the battery life of SUs. In order to design networks with high spectrum efficiency and energy efficiency, it is necessary for the SUs in CRNs to be equipped with the energy harvesting capability. However, for the SUs powered by energy harvested from wireless RF, high sampling rate is difficult to be achieved in wideband CRNs. To overcome this issue, compressive sensing (CS), which was initially proposed in [10], is introduced to wideband spectrum sensing in [11] to reduce the power consumption at SUs. As the spectrum of interest is normally underutilized in reality [12], [13], it exhibits a sparsity property in frequency domain, which makes sub-Nyquist sampling possible by implementing the CS technique at SUs. In addition, when dealing with matrices containing limited available entries, low-rank matrix completion (MC) [14] was proposed to recover the complete matrix. As the sparsity property of received signals can be transformed into low-rank property of the matrix constructed in the cooperative networks, the authors in [15] proposed to apply joint sparsity recovery and low-rank MC to reduce the requirements on sensing and transmission without degrading the sensing performance in CRNs. In order to improve robustness against channel noise, a denoised algorithm was proposed in [16] for compressive spectrum sensing at single SU and low-rank MC based spectrum sensing at multiple SUs.

A. Related Work

Some throughput optimization work has been recently developed in wireless powered communication networks. The authors in [17] considered the throughput maximization problem for both battery-free and battery-deployed cases by optimizing the time slots for energy harvesting and data transmission. In addition, recent work [18]–[20] on the CRNs powered by energy harvesting mainly focuses on the spatial throughput optimization under various constraints. The authors in [18]

Z. Qin, Y. Liu, Y. Gao and M. ElKashlan are with Queen Mary University of London, London, United Kingdom. (email: {z.qin; yuanwei.liu; yue.gao; maged.elkashlan}@qmul.ac.uk)

A. Nallanathan is with King's College London, London, United Kingdom. (email: arumugam.nallanathan@kcl.ac.uk)

considered CRNs with an energy-harvesting SU with infinite battery capacity. The goal is to design an optimal spectrum sensing policy that maximizes the expected throughput subject to an energy causality constraint and a collision constraint. In order to improve both energy efficiency and spectral efficiency, the authors in [19] considered a similar network model and the stochastic optimization problem is formulated into a constrained partially observable Markov decision process. At the beginning of each time slot, a SU needs to determine whether to remain idle so as to conserve energy, or to execute spectrum sensing to acquire knowledge of the current spectrum occupancy state. The throughput is maximized by optimizing the spectrum sensing policy and the detection threshold. The authors in [20] consider an energy constraint RF-powered CRN by optimizing the pair of the sensing duration and the sensing threshold to maximize the average throughput of the secondary network. More practically, the authors in [21] proposed to optimize the throughput of energy harvesting sensor networks by further considering the constraint on hardware memory. Furthermore, the implementation of the proposed scheme has been realized, which motivates us to bring the wireless powered networks from theory to practice.

B. Motivations and Contributions

The aforementioned work has played a vital role and laid solid foundation for developing new strategies for frame structure design. However, in [17], spectrum sensing is not considered in the frame structure design. In addition, in [18]–[20], the proposed frame structure designs mainly aim to maximize the throughput by optimizing the threshold and time slots. When considering the energy efficiency and spectrum efficiency, it is meaningful to introduce sub-Nyquist sampling to reduce the energy consumption at SUs in wireless powered CRNs. Difficult from [22], in this paper, a new frame structure is proposed for the SUs in wireless powered CRNs with different behaviours (active and inactive which are to be introduced later in Section II). With invoking CS and MC techniques, throughput is optimized at the level of an individual SU and the whole cooperative network, respectively.

The summarized contributions of this paper are illustrated as follows:

- We propose a new frame structure for the wireless powered CRNs, in which a new WPT model and the sub-Nyquist sampling are considered.
- In the WPT model, we adopt a bounded WPT scheme where each SU selects a beacon (PB) nearby with the strongest channel to harvest energy. The closed-form expressions for the power outage probability is derived. With the sub-Nyquist sampling performed at each SU, CS and low-rank MC techniques are utilized at the remote FC to recovery the original signals.
- Throughput optimisation of the proposed frame structures are formulated into two linear constrained problems with the purpose of maximising the throughput of a single SU and the whole cooperative networks, respectively. The formulated problems are solved by using three different methods to obtain the maximal achievable throughput, respectively.

- We show that the proposed frame structure design outperforms the traditional one in terms of throughput. It is noted that the multiple SUs scenario can achieve better outage performance than the single SU scenario.

C. Organisations

The rest of this paper is organised as follows. Section II describes the considered WPT model and spectrum sensing model based on the proposed frame structure. Section III presents the throughput optimization for the single SU with applying CS technique. Section IV provides the throughput optimization at the cooperative network level with adopting MC technique. Section V shows the numerical analyses of the considered network model with the purpose of optimizing throughput of single SU and the whole cooperative network, respectively. Section VI concludes this paper.

II. NETWORK MODEL

A. Network Description

We consider a CRN, where SUs are energy constrained. The whole spectrum of interest can be divided into \mathcal{I} channels. A channel is either occupied by a primary user (PU) or unoccupied. Meanwhile, there is no overlap between different channels. The number of occupied channels is assumed to be K , where $K \leq \mathcal{I}$. Each SU performs sensing on the whole spectrum. It is assumed that all SUs keep quiet as forced by protocols, e.g., at the media access control layer during spectrum sensing period. Thus the received signals from active PUs with channel noise. As shown in Fig. 1, for each SU, it is assumed that the sensing and transmission can only be scheduled by utilising energy harvested from PBs. The spatial topology of all PBs are modelled using homogeneous poisson point process (PPP) Φ_p with density λ_p . Without loss of generality, we consider that a typical SU is located at the origin in a two-dimensional plane. Each SU is equipped with a single antenna and has a corresponding receiver with fixed distance. Each PB is furnished with M antennas and maximal ratio transmission (MRT) is employed at PBs to perform WPT to the energy constrained SU. Once the spectrum holes are identified, each SU is assigned a spectrum hole by the FC to start data transmission. Here, we assume that there are enough number of spectrum holes to be allocated to SUs in a CSS network as the wideband spectrum sensing is performed at each SU. Additionally, it is assumed that the time of each frame is T . The proposed framework structure for the considered network with J ($J \geq 1$) SUs is shown in Fig. 1. The J spatially distributed SUs can be divided into two sets: *active* SUs and *inactive* SUs. Active SUs refer to SUs that can complete the spectrum sensing task with harvested energy. Inactive SUs refer to SUs without enough energy to conduct spectrum sensing. The frame structures for active SUs and inactive SUs are as follows:

- 1) Active SUs: As outlined by the blue oval in Fig. 1, the frame period for an active SU includes four time slots: 1) energy harvesting time slot, in which each SU harvests the energy from PBs during the $\alpha_1 T$ period, with α_1 being the fraction of energy harvesting in one

frame period; 2) spectrum sensing time slot, in which each SU performs sub-Nyquist sampling by applying CS techniques. The compressed measurements are then sent to a remote powerful FC during the βT period by using the harvested energy during the $\alpha_1 T$ period; 3) energy harvesting time slot for data transmission, in which each SU harvests the energy from PBs during the $\alpha_2 T$ period, with α_2 being the fraction of energy harvesting in one frame period. During this time slot, the original signals are recovered and the spectrum occupancies are determined by adopting energy detection at the FC. Subsequently, the obtained sensing decisions are sent back to corresponding SUs; and 4) data transmission slot, in which each SU performs data transmission during the $(1 - \alpha_1 - \beta - \alpha_2) T$ period. By moving the burden of spectrum recovery and decision making from energy-constrained SUs to a powerful FC, energy consumption at the SU can be reduced significantly. Additionally, SUs have a higher opportunity to performing energy harvesting;

- 2) Inactive SUs: Before performing spectrum sensing, each participating SU compares energy harvested during the first time slot E_{H_1} with E_S , where E_S is the energy consumption for spectrum sensing at the second time slot. If E_{H_1} is greater than E_S , the SU is determined as active and would continue performing spectrum sensing. If E_{H_1} is less than E_S , the SU would switch to energy harvesting model again and wait for the decision on spectrum occupancies from the FC before starting data transmission. Therefore, as outlined by the red oval in Fig. 1, the frame structure of inactive SUs only includes two time slots: $(\alpha_1 + \beta + \alpha_2) T$ for energy harvesting and the rest for data transmission. In the case of CSS, only measurements from active SUs are collected at the FC. The signals received by SUs exhibit a sparsity property that yields a matrix with low-rank property at the FC. Therefore, the full information of spectrum occupancies can be obtained by adopting the low-rank MC technique. Once the complete matrix is recovered at the FC, the final decisions on spectrum occupancies can be determined. Subsequently, the FC sends back the binary decision with the allocated spectrum hole to each SU in the CSS network.

B. Wireless Power Transfer Model

Different from the previous research works [5], [23], we consider a bounded power transfer model by assuming a minimum allowed distance d_0 between the selected PB and powered SU, which is used to avoid the singularity caused by proximity between PBs and SUs [24], [25]. If PBs are really close to the SU, the harvested energy would mathematically go to infinity [4]. It is assumed that there is no battery storage energy for future use. Therefore, all the harvested energy during energy harvesting time slots is used to perform spectrum sensing and data transmission in the current frame period [4], [6], [26]. It is also assumed that all required energy of SUs are harvested from PBs. Additionally, all PBs are

assumed to operate in the same specific frequency band for simplicity. The operation band of PBs is assumed to be isolated from that of the spectrum sensing and data transmission.

In this work, we adopt a power transfer scheme where each SU only selects one PB with the strongest channel¹ The energy harvesting channels are assumed to be quasi-static Rayleigh fading channels, where the channel coefficients are constant for each transmission block but vary independently between different blocks. At each SU, the energy harvested from the selected PB in the first and the third time slots can be obtained as follows:

$$E_{H_1} = \max_{p \in \Phi_p, \|d_p\| \geq d_0} \left\{ \|\mathbf{h}_p\|^2 L(d_p) \right\} \eta P_p \gamma T, \quad (1)$$

where γ is the ratio of the time used for energy harvesting to the total time of a frame, η is the power conversion efficiency at the SU, P_p is the transmit power of PBs. Here, due to the WPT channels are modeled as Rayleigh fading with zero mean and unit variance, the entries of $\mathbf{h}_p \in \mathcal{C}^{M \times 1}$ are independent complex Gaussian distributed with zero mean and unit variance employed to capture the effects of small-scale fading between PBs and the SU, which is because of the MRT enabled power transmission from PB with M antennas. $L(d_p) = A d_p^{-\xi}$ is the power-law path-loss exponent. The path-loss function depends on the distance d_p , a frequency dependent constant A , and an environment/terrain dependent path-loss exponent $\xi > 2$.

For the active SUs, based on (1), the maximum harvested power P_{H_1} which can be utilized for sensing at the SU is given by

$$P_{H_1} = \frac{E_{H_1}}{\beta T} = \max_{p \in \Phi_p, \|d_p\| \geq d_0} \left\{ \|\mathbf{h}_p\|^2 L(d_p) \right\} \frac{\eta P_p \alpha_1}{\beta}, \quad (2)$$

where E_{H_1} refers to the energy harvested in the first time slot.

As energy can only be stored in the current frame, the total energy for data transmission is the sum of the remaining energy in the second slot and the energy harvested in the third time slot, which is given by

$$E_{T_2} = (E_{H_1} - E_S) + E_{H_2}, \quad (3)$$

where $E_S = P_s \beta T$ with P_s being the power consumption of spectrum sensing.

Based on (1) and (3), the corresponding power for data transmission is given by

$$P_{T_2} = \frac{\max_{p \in \Phi_p, \|d_p\| \geq d_0} \left\{ \|\mathbf{h}_p\|^2 L(d_p) \right\} \eta P_p (\alpha_1 + \alpha_2) - P_s \beta}{1 - \alpha_1 - \beta - \alpha_2}. \quad (4)$$

For the inactive SUs, the harvested energy can be given by

$$E_{H_3} = \max_{p \in \Phi_p, \|d_p\| \geq d_0} \left\{ \|\mathbf{h}_p\|^2 L(d_p) \right\} \eta P_p (\alpha_1 + \beta + \alpha_2) T. \quad (5)$$

¹Note that the strongest PB is not necessarily to be the nearest one, because of the instantaneous effect of small-scale fading is also taken into considerations. To harvest energy. The other PBs would turn to sleep mode to save the energy waste. The motivation behind using this scheme is that it is capable of achieving more energy efficient power transfer compared to other possible schemes (e.g., use all of PBs for power transfer).

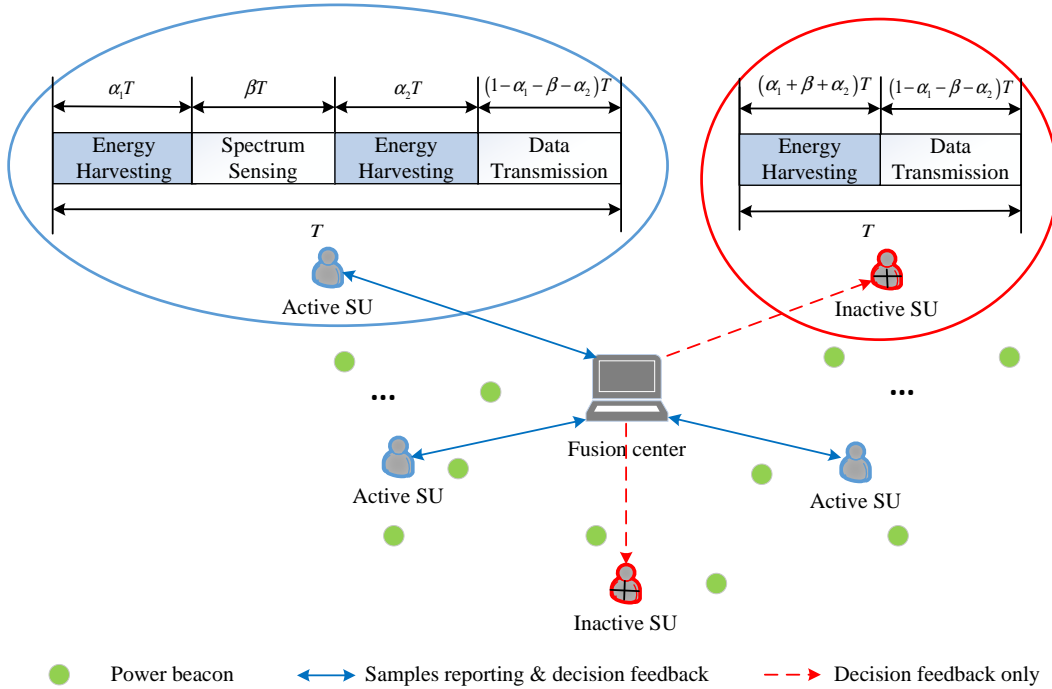


Fig. 1: Proposed frame structure design with energy harvesting, spectrum sensing and data transmission.

Based on (5), the maximum transmit power at the inactive SU can be expressed as

$$P_{H_3} = \frac{E_{H_3}}{(1 - \alpha_1 - \beta - \alpha_2)T}. \quad (6)$$

C. Spectrum Sensing Model with Sub-Nyquist Sampling

At the j th SU (SU_j) in the considered network, the received signals can be expressed as:

$$\mathbf{r}_j = \mathbf{h}_j * \mathbf{s} + \mathbf{n}_j, \quad (7)$$

where $\mathbf{s} \in \mathcal{C}^{n \times 1}$ refers to the transmitted primary signals in time domain, and $\mathbf{h}_j \in \mathcal{C}^{n \times 1}$ is the channel gain between the transmitter and receiver, and $\mathbf{n}_j \sim \mathcal{CN}(0, \sigma^2 \mathbf{I}_n)$ refers to Additive White Gaussian Noise (AWGN) with zero mean and variance σ^2 .

Based on the Nyquist sampling theory, the sampling rate is required to be no less than twice of the signal bandwidth. However, for wideband spectrum sensing, high sampling rate is difficult to achieve and also leads to high energy consumption which is challenging for energy-constrained SUs. It is noticed that the transmitted signal \mathbf{s} exhibits a sparsity property in frequency domain as a large percentage of spectrum is normally underutilized in practice. This sparsity property enables sub-Nyquist sampling at SUs without loss any signal information. The compressed measurements collected at SU_j can be given by

$$\mathbf{x}_j = \Phi_j \mathbf{r}_j = \Phi_j \mathcal{F}_j^{-1} \mathbf{r}_{fj} = \Theta_j (\mathbf{h}_{fj} \mathbf{s}_f + \mathbf{n}_{fj}), \quad (8)$$

where $\Phi_j \in \mathcal{C}^{\Lambda \times n}$ ($\Lambda < n$) is the measurement matrix utilized to collect the compressed measurements $\mathbf{x}_j \in \mathcal{C}^{\Lambda \times 1}$, and \mathbf{s}_f , \mathbf{h}_{fj} and \mathbf{n}_{fj} refer to the frequency representations of transmit

primary signals, channel coefficients, and the AWGN received at SU_j . Additionally, $\Theta_j = \Phi_j \mathcal{F}_j^{-1}$, where \mathcal{F}_j^{-1} is inverse discrete Fourier transform (IDFT) matrix. The compression ratio is defined as $\kappa = \frac{\Lambda}{n}$, ($0 \leq \kappa \leq 1$).

After the compressed measurements are collected, SUs send them to a remote FC to perform signal recovery by an error-free reporting channel. By adopting such a powerful FC, energy-constrained SUs can get rid of signal recovery process and continue harvesting more energy from PSs. At the FC, the compressed measurements \mathbf{X} can be expressed as

$$\mathbf{X} = \Theta \text{vec}(\mathbf{R}_f) = \Theta (\text{vec}(\mathbf{H}_f \mathbf{S}_f) + \mathbf{N}_f), \quad (9)$$

where $\mathbf{R}_f = [\mathbf{r}_{f1}, \mathbf{r}_{f2}, \dots, \mathbf{r}_{fJ}]$ which is in size of $n \times J$, and $\text{vec}(\mathbf{R}_f) = [r_{f1}^T, \dots, r_{fJ}^T]^T \in \mathcal{C}^{(nJ) \times 1}$. $\mathbf{S}_f \in \mathcal{C}^{n \times J}$, $\mathbf{H}_f \in \mathcal{C}^{n \times n}$ and $\mathbf{N}_f \in \mathcal{C}^{n \times J}$ refer to the matrix constructed by transmit primary signals, channel coefficients and AWGN in frequency domain. In addition, the measurement matrix is a diagonal matrix $\Theta = \text{diag}(\Theta_1, \Theta_2, \dots, \Theta_J)$ in size of $\Omega \times N$ with $\Omega = \Lambda \times J$ and $N = n \times J$. After the compressed measurements are collected at the FC, signal recovery can be formulated as a convex optimization problem. The considered network becomes a single node case when $J = 1$. Then the existing algorithm for CS can be utilized to recover the original signals. In the cooperative networks ($J > 1$), existing algorithms for low-rank MC can be implemented to complete the matrix. It has been proved that exact signal recovery can be guaranteed if the number of available measurements are no less than a minimum bound. With enough number of measurements, exact signals are obtained at the FC. Subsequently, energy detection is adopted to determine spectrum occupancies, in which the decisions are made by comparing

the energy of recovered signal with a threshold [27] defined as

$$\lambda = (\sigma_s^2 + \sigma^2) \left(1 + \frac{Q^{-1}(\bar{P}_d)}{\sqrt{n/2}} \right). \quad (10)$$

Once the sensing decisions are determined at the FC, they would be sent back to the participating SUs in the CSS network by the reporting channel to start the data transmission period.

III. THROUGHPUT OPTIMIZATION OF A SINGLE SECONDARY USER

In this section, the closed form expressions are derived for the power outage probability of spectrum sensing and data transmission, respectively. With the CS technique implemented, performance analysis with the target of maximizing throughput of each individual active SU locally is provided.

A. Power Outage Probability Analysis

We assume there exists a threshold transmit power, below which the spectrum sensing in the second slot or the data transmission in the fourth slot cannot be scheduled. We introduce power outage probability, i.e., probability that the harvested energy is not sufficient to perform spectrum sensing or carry out the data transmission at a certain desired quality-of-service (QoS) level. In practical scenarios, we expect a constant power for the data transmission. Therefore, we also denote the power threshold P_s as the sensing power in the second slot and P_t as the transmit power of the SU, respectively. The following theorem provides the exact analysis for the power outage probability at the single SU scenario.

Theorem 1. *The power outage probability of spectrum sensing P_s^{out} in the second time slot and the power outage probability of data transmission P_t^{out} in the fourth time slot can be expressed in closed-form as follows:*

$$P_\zeta^{out} = \exp \left[-\frac{\pi \lambda_p \delta}{\mu_\zeta^\delta} \sum_{m=0}^{M-1} \frac{\Gamma(m + \delta, \mu_\zeta d_0^\xi)}{m!} \right], \quad (11)$$

where $\zeta \in (s, t)$, $\mu_s = \frac{\beta P_s}{\eta P_p A \alpha_1}$, $\mu_t = \frac{P_t(1-\alpha_1-\beta-\alpha_2)+P_s\beta}{\eta P_p A(\alpha_1+\alpha_2)}$, $\delta = 2/\xi$, and $\Gamma(\cdot, \cdot)$ is the upper incomplete Gamma function.

Proof. See Appendix A. \square

Remark 1. *The derived results in Theorem 1 indicates that the power outage probability is a strictly monotonic increasing function of λ_p .*

B. Compressive Spectrum Sensing

In the scenario of CS based spectrum sensing, the original signal \mathbf{s}_f of each individual SU can be obtained respectively by solving the l_1 norm optimization problem as follows:

$$\min \|\mathbf{s}_f\|_1 \text{ s.t. } \|\Theta_j \cdot \mathbf{h}_{fj} \mathbf{s}_f - \mathbf{x}_j\|_2^2 \leq \varepsilon_j, \quad (12)$$

where ε_j is the error bound related to the noise level. This optimization problem can be solved by many existing algorithms for CS, such as by adopting many existing algorithms

such as CoSaMP [28], SpaRCS [29], etc. The computational complexity of solving the optimization problem in (12) is $O(n^3)$, which is mainly determined by the size of signals (n) to be recovered. However, this process is proposed to be performed at a powerful FC rather than the energy-constrained SUs. By doing so, energy consumption at SUs can be significantly reduced.

The performance metric of spectrum sensing can be measured by the probability of detection P_d and probability of false alarm P_f . For a target probability of detection, \bar{P}_d , with which the PUs are sufficiently protected, the threshold can be determined by (10) accordingly if the number of samples n is fixed. As a result, P_f for the spectrum sensing with single SU can be derived as follows:

$$P_f = Q \left(Q^{-1}(\bar{P}_d) \sqrt{\frac{\sigma_s^2 + \sigma^2}{\sigma^2}} + \sqrt{\frac{n}{2}} \frac{\sigma_s}{\sigma} \right), \quad (13)$$

where σ^2 and σ_s^2 refer to the noise power and signal power, respectively.

Assuming the energy cost per sample e_s in spectrum sensing is fixed, the energy consumption of spectrum sensing is proportional to the number of collected samples as given by:

$$n = \frac{\beta T P_s}{e_s}. \quad (14)$$

In fact, the number of collected samples n is determined by the sensing time slot. In this case, the energy consumed by reporting collected measurements and receiving decision results between SUs to the FC is ignored. Substituting (14) into (13), we obtain

$$P_f = \left(1 - Q \left(Q^{-1}(\bar{P}_d) \left(1 + \frac{\sigma_s^2}{\sigma^2} \right) + \sqrt{\frac{\beta T P_s}{2e_s}} \frac{\sigma_s}{\sigma} \right) \right). \quad (15)$$

C. Throughput Analysis

By considering the power outage probability, the throughput of each individual SU in a CRN can be expressed as

$$\tau = (1 - P_s^{out}) \times (1 - P_t^{out}) \times (1 - P_f) \times (1 - \alpha_1 - \beta - \alpha_2) \tau_t, \quad (16)$$

where $\tau_t = \log_2 \left(1 + \frac{P_t}{N_0} \right)$ is the throughput for the data transmission slot, and N_0 refers to the AWGN level in the data transmission channel. Here we simplify the data transmission process by not considering the fading, which means the throughput τ_t is only determined by the transmit signal-to-noise-ratio (SNR).

When implementing CS technique to achieve sub-Nyquist sampling rate at an SU, it has been proven that the exact signal recovery can be guaranteed if the number of collected measurements satisfies $\Lambda \geq C \cdot K \log(n/K)$, where C is some constant depending on each instance [30]. If the signal is recovered successfully by Λ samples, the achieved P_f would be the same as that no CS technique is implemented with n samples. Therefore, the necessary sensing time slot to achieve the same P_f can be reduced from βT to $\kappa \beta T$ with the CS technique adopted, where κ is the compression ratio at

SUs. Replacing P_s^{out} , P_t^{out} and P_f in (16) by (11) and (15) respectively, the full expression of the throughput with CS implemented can be expressed as follows:

$$\begin{aligned} \tau_{cs} = & \prod_{\zeta=\{s,t\}} \left(1 - \exp \left(- \frac{\pi \lambda_p \delta}{(\mu_\zeta^{cs})^\delta} \sum_{m=0}^{M-1} \frac{\Gamma(m + \delta, \mu_\zeta^{cs} d_0^\xi)}{m!} \right) \right) \\ & \times \left(1 - Q \left(Q^{-1}(\bar{P}_d) \left(1 + \frac{\sigma_s^2}{\sigma^2} \right) + \sqrt{\frac{\beta T P_s}{2 e_s}} \frac{\sigma_s^2}{\sigma^2} \right) \right) \\ & \times (1 - \alpha_1 - \kappa \beta - \alpha_2) \times \log_2 \left(1 + \frac{P_t}{N_0} \right). \end{aligned} \quad (17)$$

If there is no CS technique implemented at SUs, the time slot fraction for spectrum sensing follows the condition that $0 \leq \beta \leq 1$. When the CS technique is implemented at SUs, the time slot for spectrum sensing follows the condition that $CK \log(n/K) \leq \frac{\kappa \beta T P_s}{e_s} \leq n$. By combining these two conditions, the constraint for β becomes $\frac{e_s (CK \log(n/K))}{\kappa T P_s} \leq \beta \leq 1$. With the implementation of CS, the β in (11) is replaced by $\kappa \beta$.

Furthermore, the throughput can be maximized by solving the following problem:

$$\begin{aligned} (P0) : & \max_{\alpha_1, \beta, \alpha_2, P_t} \tau_{cs} & (18) \\ \text{s.t. } & C_1 : 0 \leq \alpha_1 \leq 1, \\ & C_2 : \frac{e_s (CK \log(n/K))}{\kappa T P_s} \leq \beta \leq 1, \\ & C_3 : \alpha_{2,\min} \leq \alpha_2 \leq 1, \\ & C_4 : 0 \leq 1 - \alpha_1 - \kappa \beta - \alpha_2 \leq 1, \\ & C_5 : P_{t,\min} \leq P_t \leq P_{t,\max}, \end{aligned}$$

where $\alpha_{2,\min}$ refers to the minimum time slot fraction for the third time slot. $P_{t,\min}$ and $P_{t,\max}$ refer to the allowed minimum and maximum power levels for data transmission period. Constraint C_1 bounds the time slot for energy harvesting for the first time slot. Constraint C_2 highlights the minimum time slot for compressive spectrum sensing. The lower bound of β is used to make sure the compressed sample is sufficient to guarantee exact signal recovery. Constraint C_3 ensures that the third time slot is at least enough for signal recovery at the FC and data transmission between the SU and FC. Constraint C_4 guarantees that the last time slot of a frame period is utilized for data transmission. Finally, constraint C_5 limits the transmit power level for data transmission. It is noticed that (27) is a constrained nonlinear optimization problem and the objective function is very complex. However, the constraints are linear, which motivates us to solve the optimization problem by the following three methods:

- 1) *Grid search*: The grid search algorithm for solving (27) can be described in Algorithm 1. The grid search algorithm can find out the global optimal value if the step size Δ_i ($i = 1, 2, 3, 4$) for α_1 , β , α_2 , P_t are small enough. However, the computational complexity would greatly increase if the step is set to be small enough.
- 2) *fmincon*: *fmincon* is a toolbox in MATLAB which is efficient but it may return a local optimal value.

Algorithm 1 Grid search

- 1: Initialization: $\Delta_1, \Delta_2, \Delta_3, \Delta_4$, and $\tau_{temp} = \emptyset$.
 - 2: **for all** $\alpha_1 \in (0 : \Delta_1 : 1)$, $\beta \in \left(\frac{e_s (CK \log(n/K))}{\kappa T P_s} : \Delta_2 : 1 \right)$, $\alpha_2 \in (\alpha_{2,\min} : \Delta_3 : 1)$, $P_t \in (P_{t,\min} : \Delta_4 : P_{t,\max})$ **do**
 - 3: **while** $0 \leq 1 - \alpha_1 - \kappa \beta - \alpha_2 \leq 1$ **do**
 - 4: $\tau_{temp} = [\tau_{temp}, \tau_{cs}]$ where τ_{cs} is expressed as (17).
 - 5: **end while**
 - 6: **end for**
 - 7: Return $\tau_{max} = \tau_{temp}$.
-

- 3) *Random sampling*: A set $S = \{v_1, v_2, \dots, v_Z\}$ that satisfies the conditions in (27) is generated randomly, where $v_i = (\alpha_1, \beta, \alpha_2, P_t)$ ($i \in \{1, 2, \dots, Z\}$) is a tuple of generated random samples, and Z is the number of generated tuples. The accuracy of this method depends on number of tuples Z generated for calculation. This method is efficient for solving (27) as it does not rely on advanced optimization techniques and the method of generating $(\alpha_1, \beta, \alpha_2, P_t)$ is efficient.

IV. THROUGHPUT OPTIMIZATION OF MULTIPLE SECONDARY USERS

In this section, the closed-form expressions for the power outage probability of data transmission are deprived for both the active and inactive SUs, respectively. With the implementation of MC technique, throughput of the CSS network with multiple SUs including the active and inactive ones is optimized.

A. Power Outage Probability Analysis

In this subsection, we provide power outage probability analysis for spectrum sensing and data transmission for both active and inactive SUs. In stochastic geometry networks, we usually focus on the average networks performance. As such, we first evaluate the average number of potential active users.

Corollary 1. *Based on Theorem 1, we obtain the average number of potential active users as follows:*

$$\bar{J}_{act} = J \left(1 - \exp \left[- \frac{\pi \lambda_p \delta}{\mu_s^\delta} \sum_{m=0}^{M-1} \frac{\Gamma(m + \delta, \mu_s d_0^\xi)}{m!} \right] \right). \quad (19)$$

Proof. Note that the condition that a typical single user can be active is that its harvested energy is capable of support spectrum sensing. Otherwise, it has to keep silent during the sensing slot. As such, the probability to become an active user is equal to the non-outage probability for spectrum sensing. Following the similar procedure as [31], we can obtain the average number of active users as (19). \square

Remark 2. *The derived result in Corollary 1 indicates that the average active number is a strictly monotonic increasing function of λ_p . As such, we can increase the value of \bar{J}_{act} by increasing λ_p .*

1) *Power Outage Probability of Spectrum Sensing*: In the considered CSS networks, we assume that the number of active participating SUs is J_1 . In order to guarantee there are at least J_1 number of active SUs to collect enough number measurements for exact recovery, the constraint $J_{\min} \leq J_1 \leq \bar{J}_{act}$ should be satisfied. Here, J_{\min} is defined as the minimal number of active SUs that can guarantee exact recovery. By considering the energy consumption for spectrum sensing and the minimal number of measurements required for exact recovery, the constraint on J_1 can be rewritten as $C\mu^2\nu k \log^6 \nu \leq \frac{\kappa\beta TP_s J_1}{e_s} \leq n\bar{J}_{act}$. As a result, the constraint on J_1 can be transformed into the constraint on β as follows:

$$C_6 : \frac{e_s (C\mu^2\nu k \log^6 \nu)}{\rho TP_s J_1} \leq \beta \leq 1, \quad (20)$$

where $C\mu^2\nu k \log^6 \nu$ is the lower bound of the number of observed measurements at the FC to guarantee the exact matrix recovery [32]. Here, $\nu = \max(n, J)$ and $\mu = O(\sqrt{\log \nu})$.

With the constraint on β in (20), by considering the average network performance, the power outage probability of sensing can be regarded as zero for simplicity. This behavior can be explained as follows: 1) For active SUs, it is assumed that the harvested energy from the first time slot is enough for them to take measurements for spectrum sensing. Therefore, the power outage probability of spectrum sensing for active SUs are zero; and 2) For the inactive SUs, they will not perform spectrum sensing and only transmit data during the last time slot.

2) *Power Outage Probability of Data Transmission*: For those active SUs, the power outage probability of data transmission is same that of the single SU scenario in (11). For those inactive SUs, as all the time slots before data transmission are used for energy harvesting, the power outage probability is different from (11). The following theorem provides exact analysis for the power outage probability of data transmission for both active and inactive SUs in CSS networks.

Theorem 2. *The power outage probability of data transmission at the active and inactive SUs in the fourth time slot can be expressed in closed-form as follows:*

$$P_\psi^{out} = \exp \left[-\frac{\pi\lambda_p\delta}{\mu_\psi^\delta} \sum_{m=0}^{M-1} \frac{\Gamma(m+\delta, \mu_\psi d_0^\xi)}{m!} \right] \quad (21)$$

where $\psi \in (a, i)$, $\mu_a = \frac{P_t(1-\alpha_1-\beta-\alpha_2)+P_s\beta}{\eta P_p A(\alpha_1+\alpha_2)}$, and $\mu_i = \frac{P_t(1-\alpha_1-\beta-\alpha_2)}{\eta P_p A(\alpha_1+\beta+\alpha_2)}$.

Proof. Based on (6), the power outage probability of data transmission at the active SUs is the same as P_t^{out} as given in (11) by replacing $\mu_a \rightarrow \mu_\zeta$.

Similarly, based on (6), the power outage probability of data transmission at the inactive SUs can be expressed as follows:

$$\begin{aligned} P_i^{out} &= \Pr \{P_{H_3} < P_t\} \\ &= \Pr \left\{ \max_{p \in \Phi_p, \|d_p\| \geq d_0} \left\{ \|\mathbf{h}_p\|^2 d_p^{-\xi} \right\} < \mu_i \right\}. \end{aligned} \quad (22)$$

Following the similar procedure as (A.5) and applying $\mu_i \rightarrow \mu_s$, we can obtain P_i^{out} in (21).

The proof is completed. \square

B. Matrix Completion Based Cooperative Spectrum Sensing

As the spectrum is normally underutilized in practice, the transmitted signals exhibit a sparsity property in frequency domain, which can be transformed into a low-rank property of the matrix \mathbf{X} at the FC. When only the J_1 active SUs send compressed samples to the FC, the matrix with collected measurements is incomplete at the FC. The exact matrix \mathbf{S}_f can be obtained by solving the following low-rank MC problem

$$\min \text{rank}(\mathbf{S}_f) \text{ s.t. } \|\Theta \text{vec}(\mathbf{H}_f \mathbf{S}_f) - \text{vec}(\mathbf{X})\|_2^2 \leq \varepsilon, \quad (23)$$

where $\text{rank}(\cdot)$ is the rank function of a matrix whose value is equal to the number of nonzero singular values of the matrix, and ε refers to the noise level. However, the problem in (23) is NP-hard due to the combinational nature of the function $\text{rank}(\cdot)$. It has been proved that the nuclear norm is the best convex approximation of the rank function over the unit ball of matrixes with norm no less than one [33]. Therefore, (23) can be replaced by the following convex formulation:

$$\min \|\mathbf{S}_f\|_* \text{ s.t. } \|\Theta \text{vec}(\mathbf{H}_f \mathbf{S}_f) - \text{vec}(\mathbf{X})\|_2^2 \leq \varepsilon. \quad (24)$$

The problem in (24) can be solved by multiple existing MC solvers, such as singular value decomposition [34], nuclear norm minimization [14], etc.

Once the exact matrix is recovered, energy detection can be used to determine the spectrum occupancy. In the CSS networks, as all the participating SUs send the collected samples to the FC, the data fusion is considered. Suppose the channel coefficients from the PUs to each participating SUs are known. When the channel coefficients are unknown, the weighting factor associated with the j th SU is set to be $g_j = \frac{1}{\sqrt{J}}$. By using the maximal ratio combining, probability of false alarm of the CSS networks Q_f becomes

$$Q_f = Q \left(Q^{-1}(\bar{P}_d) \sqrt{1 + \frac{\sigma_s^2}{J\sigma^2} H} + \sqrt{\frac{n}{2J}} \frac{\sigma_s^2}{\sigma^2} H \right), \quad (25)$$

where $H = \sum_{j=1}^J |\mathbf{h}_j|^2$ refers to the channel coefficients for all the participating SUs in the considered CSS networks.

C. Throughput Analysis

By applying the MC technique at the FC, β in (21) should be replaced by $\kappa\beta$. In addition, the throughput of considered CSS networks with multiple SUs can be expressed as

$$\begin{aligned} \tau_{mc} &= \prod_{j=1}^J (1 - P_\psi^{out}(j)) \times (1 - Q_f) \\ &\quad \times (1 - \alpha_1 - \kappa\beta - \alpha_2) \tau_t, \end{aligned} \quad (26)$$

where κ is defined as the compression ratio at active SUs. $\psi = a$ refers to the J_1 number of active SUs and $\psi = i$ refers to the rest of inactive SUs in the considered networks. If no MC technique is implemented at the FC and each SU is supposed to take samples at Nyquist rate, all the participating SUs will send samples to the FC. Then the throughput of the

considered networks can be given by replacing $P_\psi^{out}(j)$ in (26) with $P_a^{out}(j)$ and $\kappa = 1$. The constraints for the multiple nodes case are the same as that for the single node case except the condition for β given in (20).

The throughput can be maximized by solving the following problem:

$$\begin{aligned}
 (\text{P1}) : \quad & \max_{\alpha_1, \beta, \alpha_2, P_t} \tau_{mc} & (27) \\
 \text{s.t.} \quad & C_1 : 0 \leq \alpha_1 \leq 1, \\
 & C_3 : \alpha_{2,\min} \leq \alpha_2 \leq 1, \\
 & C_4 : 0 \leq 1 - \alpha_1 - \kappa\beta - \alpha_2 \leq 1, \\
 & C_5 : P_{t,\min} \leq P_t \leq P_{t,\max}, \\
 & C_6 : \frac{e_s (C\mu^2 \nu k \log^6 \nu)}{\rho T P_s J_1} \leq \beta \leq 1.
 \end{aligned}$$

Constraints C_1 and C_4 bound the time slot allocated for energy harvesting in first time slot and data transmission. Constraint C_3 ensures that the third time slot is enough for matrix recovery at the FC and data transmission between the SU and FC. Constraint C_5 limits the power level for data transmission. Constraint C_6 highlights the minimum time slot for compressive spectrum sensing, in which the lower bound of β is used to make sure that the number of compressed samples is sufficient to guarantee exact recovery at the FC. It is noticed that the structure of (P1) is similar as (P0). Thus we can use the similar methods to obtain the near optimal throughput for the CSS network.

V. NUMERICAL RESULTS

In the simulation, we set the frame period to be $T = 1$ s, the transmit power of PBs to be $P_p = 43$ dBm, the number of antennas of PB to be $M = 32$, the carrier frequency for power transfer to be 900 MHz, and the energy conversion efficiency of WPT to be $\eta = 0.8$. In addition, it is assumed that the target probability of detection \bar{P}_d is 90%. In this paper, we let $d_0 \geq 1$ m to make sure the path loss of WPT is equal or greater than one. In the following part, SNR = $\frac{\sigma_s^2}{\sigma_n^2}$ refers to the SNR in sensing channels. Regarding the considered Rayleigh fading model, the parameters are set as zero mean and unit variance, which is corresponding to our theoretical analysis.

A. Numerical Results on Optimizing Throughput of Single User

In this subsection, simulation results of the optimized throughput of single SU are demonstrated after the derived power outage probability in (11) and P_f in (15) are verified by Monte Carlo simulations.

Fig. 2 plots the power outage probability of spectrum sensing versus density of PBs λ_p with different power threshold P_s . The black solid and dash curves are used to represent the analytical results with $d_0 = 1$ m and $d_0 = 1.5$ m, respectively, which are both obtained from (11). Monte Carlo simulations are marked as “•” to verify our derivation. The figure shows the precise agreement between the simulation and analytical curves. One can be observed is that as density of PBs increases, the power outage probability dramatically

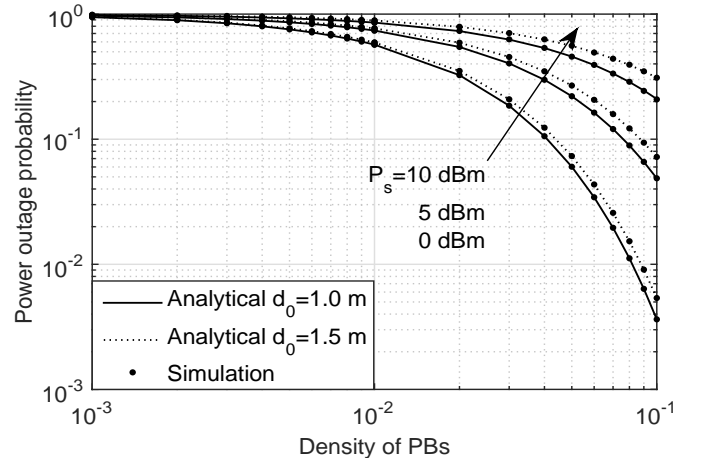


Fig. 2: Power outage probability of spectrum sensing versus density of PBs with $M = 32$, $P_p = 43$ dBm, $\alpha_1 = 0.25$, $\alpha_2 = 0.2$, and $\beta = 0.25$.

decreases, which is also corresponding to the remark we obtain from **Theorem 1**. This is because the multiuser diversity gain is improved with increasing number of PBs when charging with WPT. The figure also demonstrates that the outage occurs more frequently as the power threshold P_s and the radius of d_0 increase.

Fig. 3 plots the probability of false alarm P_f versus SNR in sensing channels with different compression ratios κ . It is observed that P_f decreases with higher SNR, which would improve the throughput of secondary network. In this case, the sparsity level is set to 12.5%, which means 12.5% of the spectrum of interest is occupied by PUs. The black solid curve is used to represent the analytical result which is obtained from (15) with enough protection to PUs being provided ($\bar{P}_d = 90\%$ is defined in the IEEE 802.22 standard about the cognitive radio [35]). Monte Carlo simulations with compression ratio $\kappa = 100\%$ are marked as “o” to verify our derivation, which represents the scenario without CS technique implemented. The figure shows precise agreement between the simulation results with $\kappa = 100\%$ and analytical curves, which is a benchmark for the following comparison. When κ is reduced to 50%, it is noticed that P_f is still well matched with the analytical result, which means the performance of spectrum sensing is not degraded when only 50% of the samples are collected at the SU. When κ is further reduced to 25%, P_f is increased, which means the signal recovery is not exact any more. As a result, wrong decisions would be made for spectrum occupancies, which leads to a higher P_f . Throughput of the CSS network would be degraded correspondingly as the chance to access vacant channels is reduced. Actually, the minimal compression ratio guaranteeing successful signal recovery is dependent on the sparsity level of signals to be recovered and the number of samples, when signals are sampled at or above Nyquist sampling rates. This is proved by Candes in [10] and out of the scope of this paper.

Fig. 4 plots the achieved throughput τ_{cs} versus the lower bound of time allocated to the third slot α_2 . Here α_2 is

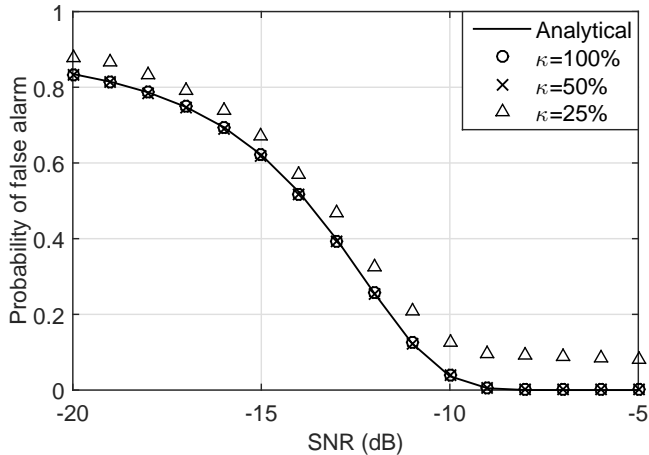


Fig. 3: Performance comparison between theoretic results for traditional energy detection and the compressive spectrum sensing under different SNR levels in sensing channels and different compression ratio κ , $\bar{P}_d = 90\%$, and sparsity level = 12.5%.

reserved for signal recovery at the FC and data transmission between the SU and the FC. In this figure, several observations are drawn as follows: 1) The maximal throughput achieved by grid search method is slight higher than that of *fmincon* method as *fmincon* relies on the initial input and may return a local optimal value. However, the accuracy of grid search method is dependent on the step sizes; 2) The random sampling method achieves lower throughput than grid search and *fmincon* methods, which demonstrates the benefits of the presented grid search and *fmincon* methods. When the generated sets increase for random sampling, the achieved throughput get closer to the optimal but the computational complexity is much increase; 3) It is seen that the optimal value of time assigned to the third slot α_2 always equals to the lower bound $\alpha_{2,\min}$. This gives a sign that the throughput can be improved if the time slot for the signal recovery at the FC and data transmission between SUs and the FC is reduced. In other words, the energy harvesting should be done mainly in the first time slot α_1 to reduce the power outage probability in the following spectrum sensing slot if the signal recovery and data transmission between the SU and FC can be promised.

Fig. 5 presents the throughput comparison between the proposed frame structure and the traditional one that does not adopting compressive spectrum sensing and remote FC to perform signal recovery. Without implementing the FC, SUs have to perform signal recovery by themselves and cannot harvest energy again after sampling. Meanwhile, in order to make decisions on spectrum occupancies, each SU has to perform energy detection locally, which introduces more energy consumption. Here, for SUs employing traditional frame structure, the time slot consumed for decision making is set to $\alpha_{2,\min}$ to simplify the comparison. The time slot required for conduct spectrum sensing at Nyquist rate is set to βT with $\beta = 0.2$. In Fig. 5, we can see that the achieved throughput is improved with decreasing compression ratio κ .

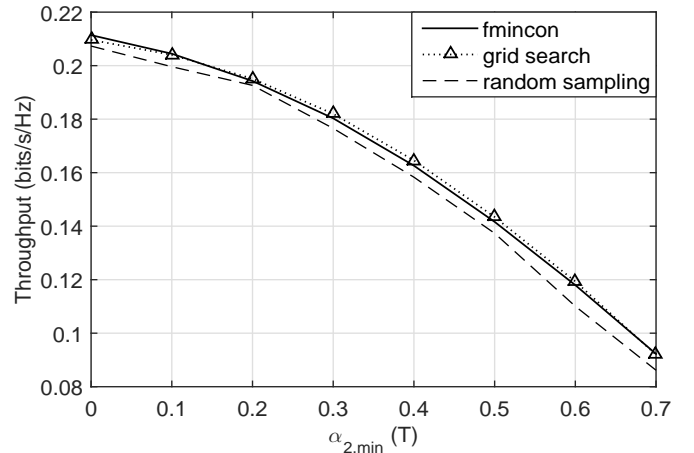


Fig. 4: Throughput of single SU τ_{cs} versus lower bound of the third time slot $\alpha_{2,\min}$, $SNR = -10$ dB, and $\kappa = 100\%$.

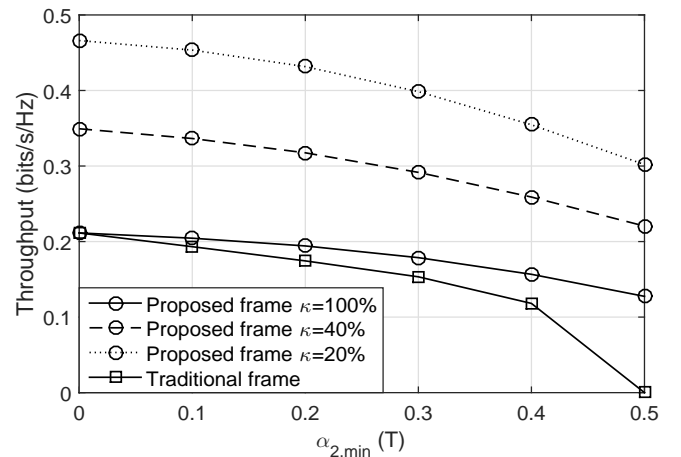


Fig. 5: Throughput comparison between the proposed frame structure and the traditional one versus lower bound of the third time slot $\alpha_{2,\min}$, $SNR = -10$ dB, and $\kappa = 100\%$, 40% and 20%.

This benefits from that more time slot becomes available for energy harvesting and data transmission when compression ratio κ decreases. It can be also noted that the achieved throughput with the traditional frame is lower than that with the proposed frame structure, even though the compression ratio κ is set to 100%. This performance degradation is caused by that the third time slot cannot be utilized for energy harvesting, as no FC is implemented for energy detection in the traditional frame structure. In a summary, we can conclude that the proposed frame structure outperforms the traditional one in terms of achieved throughput.

Fig. 6 plots the achieved throughput τ_{cs} versus lower bound of the third time slot $\alpha_{2,\min}$ and compression ratio κ when solving the problem in (27). It shows that the achieved maximal throughput increases with decreasing κ and increasing $\alpha_{2,\min}$. This behavior can be explained as follows: as κ decreases, the number of samples Λ to be collected for spectrum

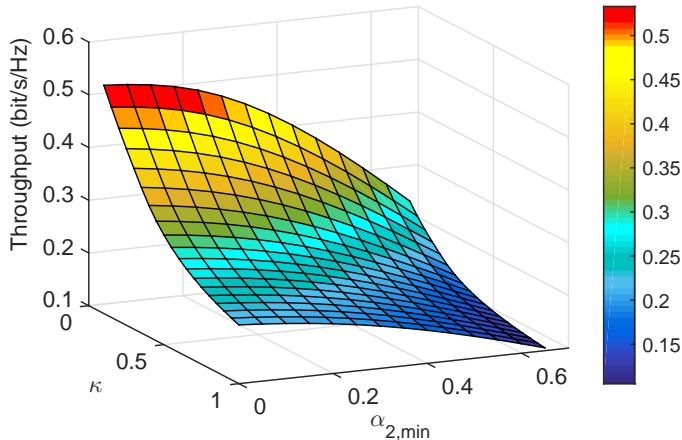


Fig. 6: Optimized throughput of single SU τ_{cs} versus lower bound of the third time slot $\alpha_{2,min}$ and compression ratio κ , and $SNR = -10$ dB in sensing channels.

sensing at an SU is reduced as the signal in original size of $N \times 1$ can be recovered from less number of measurements by utilizing the CS technique. When the time slot assigned for spectrum sensing is reduced, the energy consumption for spectrum sensing is reduced. As a result, the time which can be assigned for data transmission is increased. Therefore, the throughput of the secondary network is improved. By optimizing the transmission power P_t , the energy harvested in the current frame period would be fully utilized and the maximal throughput can be achieved accordingly. It should be noted that when the compression ratio κ is set to 100% and the lower bound of the third time slot $\alpha_{2,min}$ is zero, the achieved throughput can be regarded as that of the traditional frame structure design without considering sub-Nyquist sampling.

B. Numerical Results on Optimizing Throughput of Cooperative Spectrum Sensing Networks

In the case of optimizing the throughput of the CSS networks, the total number of participating SUs is set be to $J = 500$, including both the active and inactive SUs. Comparing the format of (P1) and (P0), we can see that both of them are linear constrained. Therefore, similar as (P0), the grid search method can be applied to obtain the optimal throughput but with non-negligible complexity, especially for the case of optimizing throughput of the whole cooperative network. The *fmincon* method can be adopted to obtain the sub-optimal throughput efficiently. In the following simulations, the *fmincon* method is utilized to solve the optimization problem (P1). In addition, as aforementioned in the introduction part, many algorithms have been proposed for the low-rank MC based cooperative spectrum sensing. With $\bar{P}_d = 90\%$, the detection performance with different compression ratios is presented in the authors' previous work in [16], which would not be demonstrated here again to reduce redundancy. In the following simulations, how the achieved throughput is influenced by parameters, such as the number of active SUs J_1 , compression ratio κ

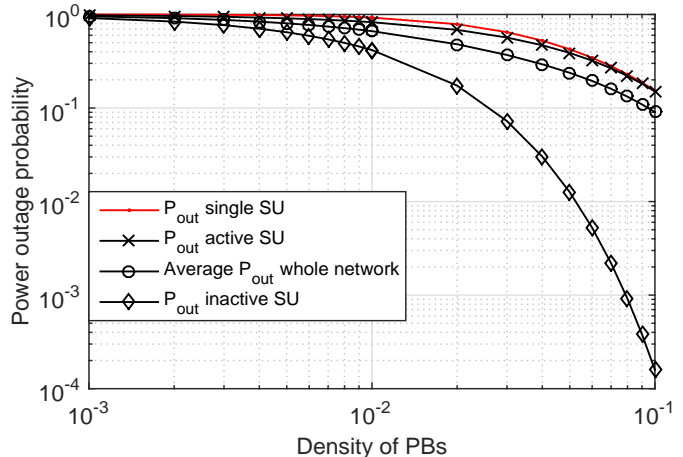


Fig. 7: Power outage probability comparison for single SU and multiple SUs with versus density of PBs, $P_s = 0$ dBm, $\alpha_1 = 0.25$, $\alpha_2 = 0.20$, and $\beta = 0.25$.

and the lower bound of the third time slot $\alpha_{2,min}$, would be demonstrated.

Fig. 7 plots the power outage probability P_{out} versus density of PBs with different power threshold P_s . In this case, the power outage probability here is for the whole system, which can be calculated as $P_{out} = 1 - (1 - P_{out}^s) \times (1 - P_{out}^t)$. Both the single SU scenario and multiple SUs scenario are illustrated in the figure. It can be observed that as density of PBs increases, the power outage probability dramatically decreases, which is caused by that the multiuser diversity gain is improved with increasing number of PBs when charging with WPT. We can also observe that the P_{out} of multiple SUs scenario is lower than that of single SU scenario. This is because the power outage probability of spectrum sensing is always zero in multiple SUs scenario, which in turn lower the power outage probability of the whole system. For the multiple SUs scenario, the P_{out} of the active SUs, inactive SUs and the average P_{out} of the CSS networks are all presented in the figure. It is noted the averaged P_{out} falls between the P_{out} of active SUs and inactive SUs, which as we expected.

Fig. 8 plots the throughput τ_{mc} averaged on per SU with different number of active SUs J_1 and different compression ratios κ at each active SU. In this case, it is assumed that the exact matrix completion can be guaranteed when the number of active SUs J_1 is in the range of 50 to 500, which refers to that the compression ratio κ changes from 10% to 100%. It shows that the average throughput achieves the best performance when the number of active SUs is set to be the minimal possible number $J_1 = 50$ in comparison with that of case $J_1 = J$. This benefits from the increasing number of inactive SUs when the number of active SUs J_1 decreases from 500 to 50. With increasing number of inactive SUs, energy consumption for spectrum sensing can be alleviated and more energy can be harvested for data transmission. It is further noticed that the achieved throughput is increased with the compression ratio κ decreasing from 75% to 20%. This benefits from that the required time slot for sub-Nyquist sensing is

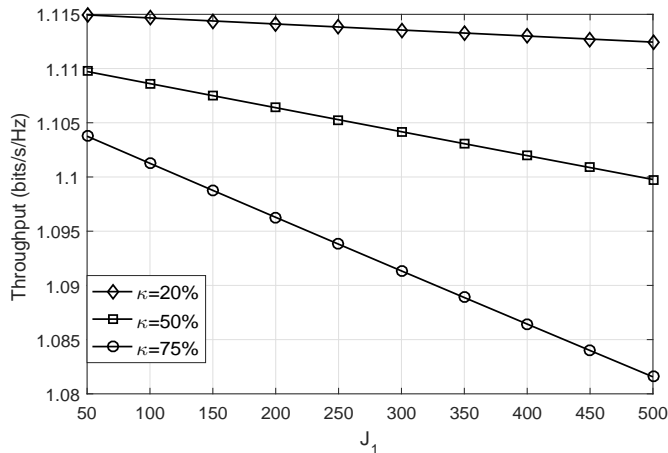


Fig. 8: Optimized throughput averaged on per SU of multiple SUs τ_{mc} versus number of active SUs J_1 and compression ratio κ , $SNR = -10$ dB in sensing channels, and $\alpha_{2,min} = 0.05$.

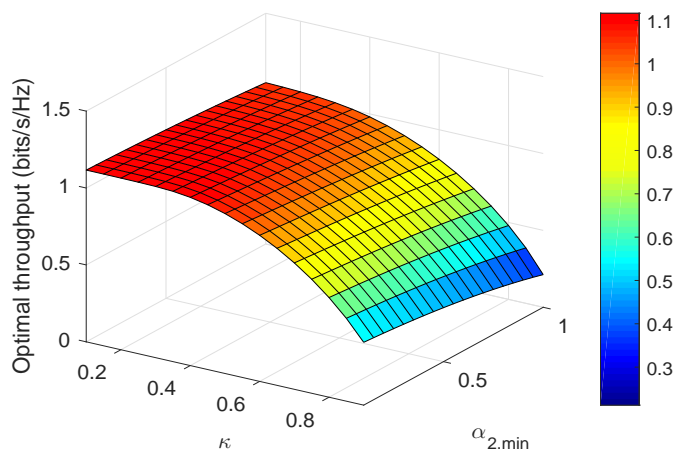


Fig. 9: Optimized throughput averaged on per SU of multiple SUs τ_{mc} versus lower bound $\alpha_{2,min}$ and compression ratio κ , and $SNR = -10$ dB in sensing channels.

reduced when the compression ratio κ is decreased.

Fig. 9 plots the achieved throughput averaged on per SU versus different compression ratio κ and lower bound for the third time slot $\alpha_{2,min}$. In this case, the number of active SUs is set to $J_1 = 300$. The achieved throughput shown in Fig. 9 is based on the condition that the exact matrix recovery can be guaranteed with the given compression ratio κ . As shown in the figure, the achieved throughput increases with decreasing compression ratio κ and $\alpha_{2,min}$. The minimal compression ratio guaranteeing the exact matrix recovery is nondeterministic, which is dependent on the rank order of the matrix to be recovered and the size of matrix to be recovered. If the rank of matrix is fixed, the larger network size J , the lower minimal compression ratio which can guarantee the exact matrix recovery.

VI. CONCLUSIONS

In this paper, a wireless powered cognitive radio (CR) network has been considered. In the considered networks, while protecting the primary users, we proposed a new frame structure including energy harvesting, spectrum sensing, energy harvesting and data transmission. In the considered network with the proposed frame structure, closed-form expressions in terms of power outage probability was derived for the proposed wireless power transfer (WPT) scheme. Additionally, sub-Nyquist sampling was performed at secondary users (SUs) to reduce the energy consumption during spectrum sensing. The compressive sensing and matrix completion techniques were adopted at a remote fusion center to perform the signal recovery for detection making on spectrum occupancy. By optimizing the four time slots, throughput of an individual SU and the whole cooperative networks were maximized, respectively. Simulation results showed that the throughput can be improved by adopting the proposed new frame structure design. We conclude that by carefully tuning the parameters for different time slots and transmit power, WPT can be used along with sub-Nyquist sampling to provide a high quality of throughput performance for CR network, with significantly energy computation reduction at power-limited SUs.

APPENDIX A: PROOF OF THEOREM 1

Based on (2), the power outage probability of spectrum sensing can be expressed as

$$\begin{aligned} P_s^{out} &= \Pr \{P_{H_1} \leq P_s\} \\ &= E_{\Phi_p} \left\{ \prod_{p \in \Phi_p, \|d_p\| \geq d_0} \Pr \left\{ \|\mathbf{h}_p\|^2 \leq d_p^\xi \mu_s \right\} \right\} \\ &= E_{\Phi_p} \left\{ \prod_{p \in \Phi_p, \|d_p\| \geq d_0} F_{\|\mathbf{h}_p\|^2} (d_p^\xi \mu_s) \right\}, \quad (\text{A.1}) \end{aligned}$$

where $F_{\|\mathbf{h}_p\|^2}$ is the cumulative density function (CDF) of $\|\mathbf{h}_p\|^2$. As aforementioned in Section II, each channel element of \mathbf{h}_p follows Rayleigh fading, which is independent complex Gaussian distributed with zero mean and unit variance. As a consequence, $\|\mathbf{h}_p\|^2$ follows a chi-squared distribution, which is given by

$$F_{\|\mathbf{h}_p\|^2} (x) = 1 - \frac{\Gamma(M, x)}{\Gamma(M)}. \quad (\text{A.2})$$

Given the fact that M is an integer value, with the aid of [36, Eq. (8.832.2)], (A.2) can be expressed as

$$F_{\|\mathbf{h}_p\|^2} (x) = 1 - e^{-x} \left(\sum_{m=0}^{M-1} \frac{x^m}{m!} \right). \quad (\text{A.3})$$

Applying the moment generating function, we rewrite (A.1) as

$$P_s^{out} = \exp \left[-\lambda_p \int_{R^2} \left(1 - F_{\|\mathbf{h}_p\|^2} (d_p^\xi \mu_s) \right) dd_p \right]. \quad (\text{A.4})$$

Then changing to polar coordinates and substituting (A.3) into (A.4), we obtain

$$P_s^{out} = \exp \left[-2\pi\lambda_p \sum_{m=0}^{M-1} \frac{\mu_s^m \int_{d_0}^{\infty} d_p^{m\xi+1} e^{-\mu_s d_p^\xi} dd_p}{m!} \right]. \quad (\text{A.5})$$

Applying [36, Eq. (3.381.9)] to calculate the integral, we obtain (11).

Similarly, based on (4), the power outage probability of data transmission P_t^{out} can be expressed as follows:

$$P_t^{out} = \Pr \{P_{T_2} \leq P_t\} \\ = \Pr \left\{ \max_{p \in \Phi_p, \|d_p\| \geq d_0} \left\{ \|\mathbf{h}_p\|^2 d_p^{-\xi} \right\} \leq \mu_t \right\}. \quad (\text{A.6})$$

Following the similar procedure as (A.5) and applying $\mu_t \rightarrow \mu_s$, we obtain P_t^{out} in (11).

The proof is completed.

REFERENCES

- [1] V. Raghunathan, S. Ganeriwal, and M. Srivastava, "Emerging techniques for long lived wireless sensor networks," *IEEE Commun. Mag.*, vol. 44, no. 4, pp. 108–114, May 2006.
- [2] T. Le, K. Mayaram, and T. Fiez, "Efficient far-field radio frequency energy harvesting for passively powered sensor networks," *IEEE J. Solid-State Circuits*, vol. 43, no. 5, pp. 1287–1302, May 2008.
- [3] R. Zhang and C. K. Ho, "MIMO broadcasting for simultaneous wireless information and power transfer," *IEEE Trans. Commun.*, vol. 12, no. 5, pp. 1989–2001, Mar. 2013.
- [4] K. Huang and V. K. Lau, "Enabling wireless power transfer in cellular networks: architecture, modeling and deployment," *IEEE Trans. Wireless Commun.*, vol. 13, no. 2, pp. 902–912, Feb. 2014.
- [5] Y. Liu, L. Wang, S. Zaidi, M. Elkashlan, and T. Duong, "Secure D2D communication in large-scale cognitive cellular networks: A wireless power transfer model," *IEEE Trans. Commun.*, vol. 64, no. 1, pp. 329–342, Jan. 2016.
- [6] Z. Ding, S. M. Perlaza, I. Esnaola, and H. V. Poor, "Power allocation strategies in energy harvesting wireless cooperative networks," *IEEE Trans. Wireless Commun.*, vol. 13, no. 2, pp. 846–860, Jan. 2014.
- [7] Y. Liu, Z. Ding, M. Elkashlan, and H. V. Poor, "Cooperative non-orthogonal multiple access with simultaneous wireless information and power transfer," *IEEE J. Sel. Areas Commun.*, vol. 34, no. 4, April 2016.
- [8] X. Huang, T. Han, and N. Ansari, "On green-energy-powered cognitive radio networks," *IEEE Commun. Surveys Tuts.*, vol. 17, no. 2, pp. 827–842, Second quarter 2015.
- [9] X. Lu, P. Wang, D. Niyato, and E. Hossain, "Dynamic spectrum access in cognitive radio networks with RF energy harvesting," *IEEE Wireless Commun.*, vol. 21, no. 3, pp. 102–110, Jun. 2014.
- [10] E. Candes, "Compressive sampling," in *Proc. of the International Congress of Mathematicians*, vol. 3, Madrid, Spain, Aug. 2006, pp. 1433–1452.
- [11] Z. Tian and G. Giannakis, "Compressed sensing for wideband cognitive radios," in *Proc. of IEEE International Conference on Acoustics, Speech and Signal Processing (ICASSP)*, vol. 4, Honolulu, HI, Apr. 2007, pp. 1357–1360.
- [12] P. Kolodzy and I. Avoidance, "Spectrum policy task force," *Federal Commun. Comm., Washington, DC, Rep. ET Docket*, no. 02-135, 2002.
- [13] UK Office of Communications (Ofcom), "Statement on Cognitive Access to Interleaved Spectrum," Jul. 2009. [Online]. Available: <http://stakeholders.ofcom.org.uk/binaries/consultations/cognitive/statement/statement.pdf>
- [14] E. J. Candès and B. Recht, "Exact matrix completion via convex optimization," *Foundations of Computational mathematics*, vol. 9, no. 6, pp. 717–772, 2009.
- [15] J. Meng, W. Yin, H. Li, E. Hossain, and Z. Han, "Collaborative spectrum sensing from sparse observations in cognitive radio networks," *IEEE J. Sel. Areas Commun.*, vol. 29, no. 2, pp. 327–337, Feb. 2011.
- [16] Z. Qin, Y. Gao, M. Plumbley, and C. Parini, "Wideband spectrum sensing on real-time signals at sub-Nyquist sampling rates in single and cooperative multiple nodes," *IEEE Trans. Signal Process.*, vol. 64, no. 12, pp. 3106–3117, Jun. 2016.
- [17] Y. L. Che, L. Duan, and R. Zhang, "Spatial throughput maximization of wireless powered communication networks," *IEEE J. Sel. Areas Commun.*, vol. 33, no. 8, pp. 1534–1548, Jul. 2015.
- [18] S. Park, H. Kim, and D. Hong, "Cognitive radio networks with energy harvesting," *IEEE Trans. Wireless Commun.*, vol. 12, no. 3, pp. 1386–1397, Mar. 2013.
- [19] S. Park and D. Hong, "Optimal spectrum access for energy harvesting cognitive radio networks," *IEEE Trans. Wireless Commun.*, vol. 12, no. 12, pp. 6166–6179, Nov. 2013.
- [20] W. Chung, S. Park, S. Lim, and D. Hong, "Spectrum sensing optimization for energy-harvesting cognitive radio systems," *IEEE Trans. Wireless Commun.*, vol. 13, no. 5, pp. 2601–2613, Apr. 2014.
- [21] S. Yang, Y. Tahir, P. Chen, M. Alan, and J. McCann, "Distributed optimization in energy harvesting sensor networks with dynamic in-network data processing," in *Proceeding of INFOCOM*, San Francisco, CA, Apr. 2016.
- [22] Z. Qin, Y. Liu, Y. Gao, M. Elkashlan, and A. Nallanathan, "Throughput analysis for compressive spectrum sensing with wireless power transfer," in *Proceeding of IEEE Global Communication Conference (GLOBECOM)*, San Diego, CA, Dec. 2015, pp. 1–6.
- [23] Y. Liu, L. Wang, S. Zaidi, M. Elkashlan, and T. Duong, "Secure D2D communication in large-scale cognitive cellular networks with wireless power transfer," in *Proceeding IEEE International Conference on Communications (ICC)*, London, UK, June 2015, pp. 4309–4314.
- [24] J. Venkataraman, M. Haenggi, and O. Collins, "Shot noise models for outage and throughput analyses in wireless ad hoc networks," in *Proceeding of Military Communications Conference (MILCOM)*, Oct. 2006, pp. 1–7.
- [25] F. Baccelli, B. Blaszczyzyn, and P. Muhlethaler, "An aloha protocol for multihop mobile wireless networks," *IEEE Trans. Inf. Theory*, vol. 52, no. 2, pp. 421–436, Feb 2006.
- [26] Y. Liu, S. A. Mousavifar, Y. Deng, C. Leung, and M. Elkashlan, "Wireless energy harvesting in a cognitive relay network," *IEEE Trans. Wireless Commun.*, vol. 15, no. 4, pp. 2498–2508, Apr. 2016.
- [27] Y.-C. Liang, Y. Zeng, E. Peh, and A. T. Hoang, "Sensing-throughput tradeoff for cognitive radio networks," *IEEE Trans. Wireless Commun.*, vol. 7, no. 4, pp. 1326–1337, Apr. 2008.
- [28] D. Needell and J. A. Tropp, "Cosamp: Iterative signal recovery from incomplete and inaccurate samples," *Applied and Computational Harmonic Analysis*, vol. 26, no. 3, pp. 301–321, 2009.
- [29] A. E. Waters, A. C. Sankaranarayanan, and R. Baraniuk, "Sparcs: Recovering low-rank and sparse matrices from compressive measurements," in *Advances in neural information processing systems*, 2011, pp. 1089–1097.
- [30] E. J. Candès and M. B. Wakin, "An introduction to compressive sampling," *IEEE Signal. Proc. Mag.*, vol. 25, no. 2, pp. 21–30, Mar. 2008.
- [31] H. S. Jo, Y. J. Sang, P. Xia, and J. G. Andrews, "Heterogeneous cellular networks with flexible cell association: A comprehensive downlink SINR analysis," *IEEE Trans. Wireless Commun.*, vol. 11, no. 10, pp. 3484–3495, Oct. 2012.
- [32] E. J. Candès and Y. Plan, "Matrix completion with noise," *IEEE Proceedings*, vol. 98, no. 6, pp. 925–936, Mar. 2010.
- [33] M. Fazel, "Matrix rank minimization with applications," Ph.D. dissertation, Stanford University, Mar. 2002.
- [34] P. Drineas, I. Kerenidis, and P. Raghavan, "Competitive recommendation systems," in *Proc. of the thirty-fourth annual ACM symposium on theory of computing*, 2002, pp. 82–90.
- [35] M. Sherman, A. N. Mody, R. Martinez, C. Rodriguez, and R. Reddy, "IEEE standards supporting cognitive radio and networks, dynamic spectrum access, and coexistence," *IEEE Commun. Mag.*, vol. 46, no. 7, pp. 72–79, 2008.
- [36] I. S. Gradshteyn and I. M. Ryzhik, *Table of Integrals, Series and Products*, 6th ed. New York, NY: Academic Press, 2000.